Acta Mech 223, 387–394 (2012)
DOI 10.1007/s00707-011-0558-z

Ali Darvishian · Hamid Moeenfard · Mohammad Taghi Ahmadian · Hassan Zohoor

A coupled two degree of freedom pull-in model for micromirrors under capillary force

Received: 19 April 2011 / Published online: 1 November 2011

Abstract The current paper presents a two degree of freedom model for the problem of micromirrors under capillary force. The principal of minimum potential energy is employed for finding the equilibrium equations governing the deflection and the rotation of the micromirror. Then, using the implicit function theorem, a coupled bending–torsion model is presented for pull-in characteristics of micromirrors under capillary force and the concept of instability mode is introduced. It is observed that with increasing ratio of bending and torsion stiffness, the dominant instability mode changes from bending mode to the torsion mode. In order to verify the accuracy of the coupled model, static behavior of a group of micromirrors is investigated both analytically using the presented model and numerically using the commercial finite element software ANSYS. It is observed that results of the coupled model match well with the results of finite element simulations, but they both deviate considerably from the results of the pure torsion model. The presented coupled model can be used for safe and stable design of micromirrors under capillary force.

1 Introduction

The technology of MEMS devices has experienced lots of progress. Their low manufacturing cost, batch production, light weight, small size, durability, low energy consumption and compatibility with integrated circuits make them extremely attractive [1,2]. Successful MEMS devices rely not only on well-developed fabrication technologies but also on the knowledge of device behavior, based on which a favorable structure of the device can be forged [3]. The important role of MEMS devices in optical systems has initiated the development of a new class of MEMS called MicroOptoElectroMechanical Systems (MOEMS), which mainly include micromirrors and torsional microactuators. These devices have found a variety of applications such as digital micromirror devices (DMD) [4], optical switches [5], micro scanning mirrors [6] and optical cross-connects [7,8].

The existence of a liquid bridge between two objects results in a capillary force [9]. Their existence even in low relative humidity is observed experimentally [10]. Parallel plate MEMS actuators are conventionally fabricated by forming a layer of a plate or beam material on the top of a sacrificial layer of another material and wet etching the sacrificial layer. In this process, a capillary force can be easily formed and in the case of poor design, the structure will collapse and adhere to the substrate. Thus, investigating the effect of capillary force on micromirrors is extremely important in their design and fabrication.

A. Darvishian · H. Moeenfard
School of Mechanical Engineering, Sharif University of Technology, Azadi Ave., Tehran, Iran
E-mail: alidarvishian@gmail.com

M. T. Ahmadian (✉) · H. Zohoor
Center of Excellence in Design, Robotics and Automation, School of Mechanical Engineering,
Sharif University of Technology, Azadi Ave., Tehran, Iran
E-mail: ahmadian@mech.sharif.edu

The effect of capillary force on MEMS devices has been investigated by many researchers. Mastrangelo and Hsu [11,12] studied the stability and adhesion of thin micromechanical structures under capillary force, theoretically and experimentally. Moeenfard et al. [13] studied the effect of capillary force on the static pull-in instability of fully clamped microplates. The effects of capillary force on the static and dynamic behavior of atomic force microscopes (AFM) are widely assessed [14–16]. Recently, the instability of torsional MEMS/NEMS microactuators under capillary force was investigated by Guo et al. [17], but in their model, the bending effect of the supporting torsion beams was not considered. On the other hand, Huang et al. [18] showed that torsion models for a micromirror cannot accurately predict the stability limits of electrostatically actuated micromirrors. In this paper, it will be shown that the same concern exists for the micromirrors under the effect of capillary force, and neglecting the bending effect can lead to a considerable error in the prediction of stable limits of micromirrors under capillary force.

2 Problem formulation

2.1 Coupled bending–torsion model

The micromirror shown in Fig. 1 is considered. The capillary pressure underneath the mirror is [13]

$$P_{\text{Cap}} = \frac{2\gamma \cos\theta_c}{h - z - x\theta}, \tag{1}$$

where γ is the surface energy of the liquid, θ_c is the contact angle between liquid and solid surface, h is the initial distance between the mirror and the underneath substrate, z is the vertical deflection of the torsion beams, and θ is the rotation angle of the mirror. Capillary pressure can be expressed in terms of dimensionless variables in the following manner:

$$P_{\text{Cap}} = \frac{h}{WL} \cdot \frac{\eta}{1 - \Delta - \frac{x}{L}\Theta}, \tag{2}$$

where $\eta = 2\gamma \cos\theta_c WL/h^2$ is called instability number, and W and L are the width and length of the micromirror, respectively, and $\Delta = z/h$ and $\Theta = \theta/\theta_0$ are normalized parameters with respect to h and the maximum physically possible rotation angle $\theta_0 = h/L$ of the micromirror.

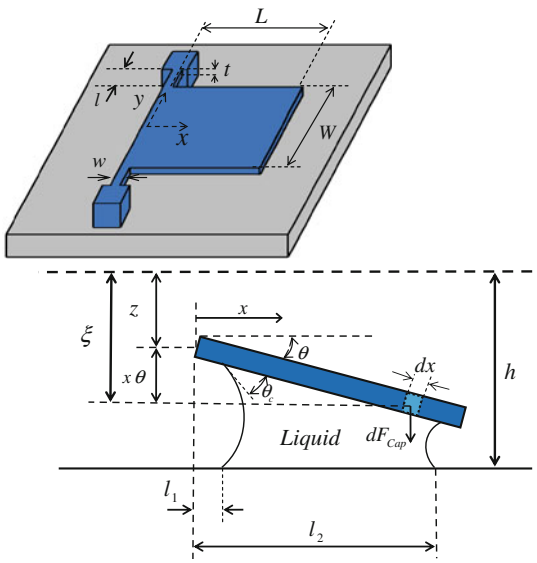

Fig. 1 Schematic view of a micromirror under the effect of capillary force

The differential capillary force applied to a differential surface area $W\mathrm{d}x$ of the mirror shown in Fig. 1 can be calculated from the capillary pressure as:

$$\mathrm{d}F_{\mathrm{Cap}} = P_{\mathrm{Cap}} W \mathrm{d}x = \frac{h}{L} \frac{\eta}{1 - \Delta - \frac{x}{L}\Theta} \mathrm{d}x. \tag{3}$$

The total external work done on the micromirror by the capillary force is:

$$W_e = \int \int \mathrm{d}F_{\mathrm{Cap}} \mathrm{d}\xi, \tag{4}$$

where $\xi = z + x\theta$ is a position parameter shown in Fig. 1. Using Eq. (3) and $\mathrm{d}\xi = \mathrm{d}z + x\mathrm{d}\theta$ for a given element position x, i.e., $\mathrm{d}x = 0$, in Eq. (4) gives

$$W_e = \frac{1}{2}\eta\Psi, \tag{5}$$

where

$$\begin{aligned}\Psi(\Theta, \Delta) &= \frac{2h^2}{L} \int_{l_1}^{l_2} \left(\int_0^{\Delta} \frac{1}{1 - \Delta' - \frac{x}{L}\Theta} \mathrm{d}\Delta' + \int_0^{\Theta} \frac{1}{1 - \Delta - \frac{x}{L}\Theta'} \frac{1}{L} x \mathrm{d}\Theta' \right) \mathrm{d}x \\ &= 2h^2 \left(\int_0^{\Delta} \frac{-\ln \frac{1-\Delta'-\beta\Theta}{1-\Delta'-\alpha\Theta}}{\Theta} \mathrm{d}\Delta' + \int_0^{\Theta} \frac{-\Theta'(\beta - \alpha) + (\Delta - 1)\ln \frac{1-\Delta-\beta\Theta'}{1-\Delta-\alpha\Theta'}}{\Theta'^2} \mathrm{d}\Theta' \right).\end{aligned} \tag{6}$$

In Eq. (6), l_1 and l_2 are the start and end point of the capillary bridge underneath the mirror as illustrated in Fig. 1, and $\alpha = l_1/L$ and $\beta = l_2/L$ are the normalized values of l_1 and l_2, respectively. The potential energy stored in the torsion beams due to the rotation θ and deflection z is

$$U = \frac{1}{2}S_0\theta^2 + \frac{1}{2}K_0 z^2 = \frac{1}{2}S_0\theta_0^2\Theta^2 + \frac{1}{2}K_0 h^2 \Delta^2, \tag{7}$$

where S_0 and K_0 are the overall torsional and vertical stiffness of the two torsion beams and can be calculated from the length l of each torsion beam, the shear modulus G and Young's modulus E, the polar moment of inertia I_p and the second moment of inertia I_b of the beam's cross-section as

$$S_0 = \frac{2GI_p}{l}, \quad K_0 = \frac{24EI_b}{l^3}. \tag{8}$$

For beams with rectangular cross-section, I_b and I_p can be computed according to [18]:

$$I_b = \frac{1}{12}wt^3, \quad I_p = \frac{1}{3}tw^3 - \frac{64}{\pi^5}w^4 \sum_{n=1}^{\infty} \frac{1}{(2n-1)^5} \tanh \frac{(2n-1)\pi t}{2w}, \tag{9}$$

where t and w are the length and width of the beam's cross-section, respectively. The total potential energy [19] of the system is:

$$\Pi = U - W_e. \tag{10}$$

At equilibrium state, the variation of Π vanishes, i.e.,

$$\delta\Pi = \frac{\partial\Pi}{\partial\Delta}\delta\Delta + \frac{\partial\Pi}{\partial\Theta}\delta\Theta = 0. \tag{11}$$

With arbitrary variations $\delta\Delta$ and $\delta\Theta$ for the independent deflection and rotation variables, one finds with Eqs. (5) and (10) the following equilibrium equations:

$$\Xi_{T1}(\Theta, \Delta) = \frac{\partial \prod}{\partial\Theta} = \frac{\partial U}{\partial\Theta} - \frac{1}{2}\eta\frac{\partial\Psi}{\partial\Theta} = 0, \tag{12}$$

$$\Xi_{T2}(\Theta, \Delta) = \frac{\partial \prod}{\partial\Delta} = \frac{\partial U}{\partial\Delta} - \frac{1}{2}\eta\frac{\partial\Psi}{\partial\Delta} = 0. \tag{13}$$

Substituting Eqs. (6) and (7) into the equilibrium conditions (12) and (13) yields

$$\Xi_{T1}(\Theta, \Delta)/h^2 = K_t\Theta + \frac{\eta}{\Theta}\left(\beta - \alpha + \frac{1-\Delta}{\Theta}\ln\left(\frac{1-\Delta-\beta\Theta}{1-\Delta-\alpha\Theta}\right)\right) = 0, \tag{14}$$

$$\Xi_{T2}(\Theta, \Delta)/h^2 = K_b\Delta + \frac{\eta}{\Theta}\ln\left(\frac{1-\Delta-\beta\Theta}{1-\Delta-\alpha\Theta}\right) = 0, \tag{15}$$

where $K_t = S_0/L^2$, $K_b = K_0$.

With increasing values of η, the values of Δ and Θ are increased. At the pull-in state, η has its maximum value. Applying the implicit function theorem [20,21] to Eqs. (14) and (15), a unique solution $\Theta(\eta)$ and $\Delta(\eta)$ gets lost, i.e., the pull-in state is reached, when the determinant

$$\begin{vmatrix} \frac{\partial \Xi_{T1}}{\partial \Theta} & \frac{\partial \Xi_{T1}}{\partial \Delta} \\ \frac{\partial \Xi_{T2}}{\partial \Theta} & \frac{\partial \Xi_{T2}}{\partial \Delta} \end{vmatrix} = 0. \tag{16}$$

Applied to Eqs. (14), (15) and after eliminating η, the following equations for the pull-in state are obtained:

$$\ln\left(\frac{1-\Delta_p-\beta\Theta_p}{1-\Delta_p-\alpha\Theta_p}\right) - \Upsilon\frac{\Delta_p}{\Theta_p}\left(\beta-\alpha+\frac{1-\Delta_p}{\Theta_p}\ln\left(\frac{1-\Delta_p-\beta\Theta_p}{1-\Delta_p-\alpha\Theta_p}\right)\right) = 0, \tag{17}$$

$$\begin{aligned} &\left(\frac{3(1-\Delta_p)}{\Theta_p}\ln\left(\frac{1-\Delta_p-\beta\Theta_p}{1-\Delta_p-\alpha\Theta_p}\right) - \frac{(1-\Delta_p)^2(\alpha-\beta)}{(1-\Delta_p-\alpha\Theta_p)(1-\Delta_p-\beta\Theta_p)} - 2(\alpha-\beta)\right) \\ &\left(\ln\left(\frac{1-\Delta_p-\beta\Theta_p}{1-\Delta_p-\alpha\Theta_p}\right) + \frac{\Delta_p\Theta_p(\alpha-\beta)}{(1-\Delta_p-\alpha\Theta_p)(1-\Delta_p-\Theta_p)}\right) \\ &-\Delta_p\Theta_p\left(\frac{(1-\Delta_p)(\alpha-\beta)}{(1-\Delta_p-\alpha\Theta_p)(1-\Delta_p-\beta\Theta_p)} - \frac{1}{\Theta_p}\ln\left(\frac{1-\Delta_p-\beta\Theta_p}{1-\Delta_p-\alpha\Theta_p}\right)\right)^2 = 0, \end{aligned} \tag{18}$$

where $\Upsilon = K_b/K_t$ is a parameter characterizing the stiffness ratio of bending and torsion. The value of η at the pull-in state (Θ_P, Δ_p) is calculated from Eq. (13) as

$$\eta_P = 2\left.\frac{\frac{\partial U}{\partial \Delta}}{\frac{\partial \Psi}{\partial \Delta}}\right|_{(\Theta_p, \Delta_p)} = \frac{K_t\Upsilon\Delta_P\Theta_P}{\ln\left(\frac{1-\Delta_p-\alpha\Theta_p}{1-\Delta_p-\beta\Theta_p}\right)}. \tag{19}$$

It will be shown later that for small Υ, i.e., bending stiffness is less effective than torsion stiffness, the dominant instability mode of the micromirror will be the bending mode, otherwise the dominant instability mode will be the torsion mode.

2.2 Pure torsion model

If bending of the torsion beams is not considered in the formulation, i.e., $\Delta = z/h = 0$, the total potential energy (10) is only a function of Θ and the equilibrium equation can formally be obtained by setting Δ equal to zero in Eq. (14):

$$\Xi_{T1}(\Theta)/\left(h^2K_t\right) = \Theta + \frac{\eta'}{\Theta}\left(\beta-\alpha+\frac{1}{\Theta}\ln\left(\frac{1-\beta\Theta}{1-\alpha\Theta}\right)\right) = 0, \tag{20}$$

where $\eta' = \eta/K_t$. The pull-in condition is then reduced to

$$\frac{\mathrm{d}\eta'}{\mathrm{d}\Theta} = 0. \tag{21}$$

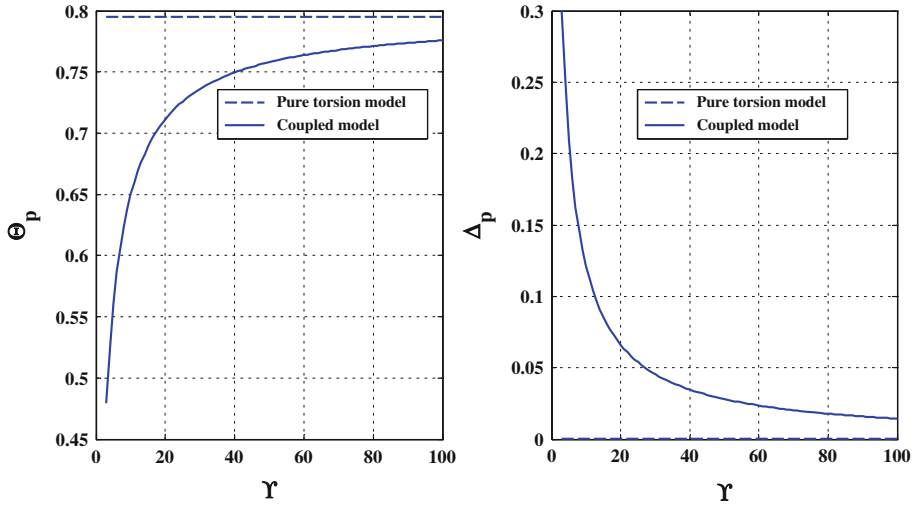

Fig. 2 Dependency of the normalized pull-in angle Θ_P and pull-in displacement Δ_P of the micromirror on Υ at $\alpha = 0.2$ and $\beta = 0.8$

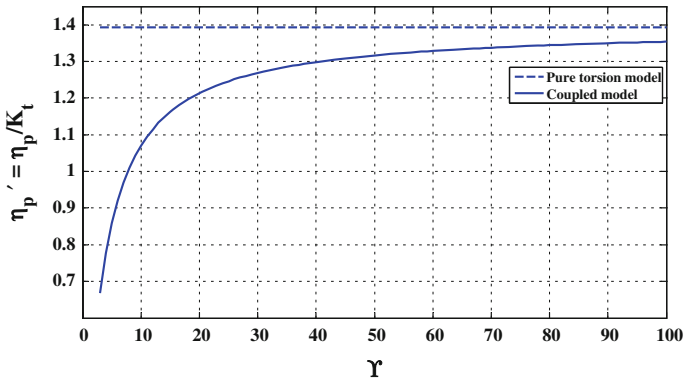

Fig. 3 Values of $\eta' = \eta/K_t$ at the pull-in point against Υ at $\alpha = 0.2$ and $\beta = 0.8$

3 Results and discussion

Figure 2 shows the dependency of the normalized pull-in angle Θ_P and normalized pull-in displacement Δ_p of the micromirror versus Υ for $\alpha = 0.2$ and $\beta = 0.8$. It is observed that with increasing values of Υ, the value of Θ_P asymptotically approaches the value of the pull-in angle predicted by the torsion model and the value of Δ_P asymptotically approaches 0. Thus, for low values of Υ, the torsion model deviates considerably from the bending model; that is why neglecting the bending effect leads to significant errors in predicting the pull-in angle Θ_P of the mirror.

In Fig. 3, the values of the normalized instability number $\eta' = \eta/K_t$ at the pull-in point are plotted against Υ for both torsion and coupled model at $\alpha = 0.2$ and $\beta = 0.8$. This figure implicitly indicates that at small values of Υ, the predicted value η' of the torsion model is significantly higher than that of the coupled model, and thus the torsion model overestimates the instability limits of the mirror; its related results cannot be trusted for a safe and stable design.

In order to investigate the effects of α and β on the pull-in response, the pull-in angle Θ_P and pull-in displacement Δ_P of the micromirror are plotted against α for different values of β for both pure torsion and coupled model at $\Upsilon = 10$. It is observed that with increasing values of α and/or β, pull-in angle Θ_P and pull-in displacement Δ_P decrease.

In Fig. 5, the related values of η'_p of Fig. 4 are plotted against α. This figure shows that with decreasing values of α and/or increasing values of β, the stability limit of the micromirror is reduced and pull-in would occur at lower values of η'. Since curves related to the pure torsion model in Fig. 5 are above the related

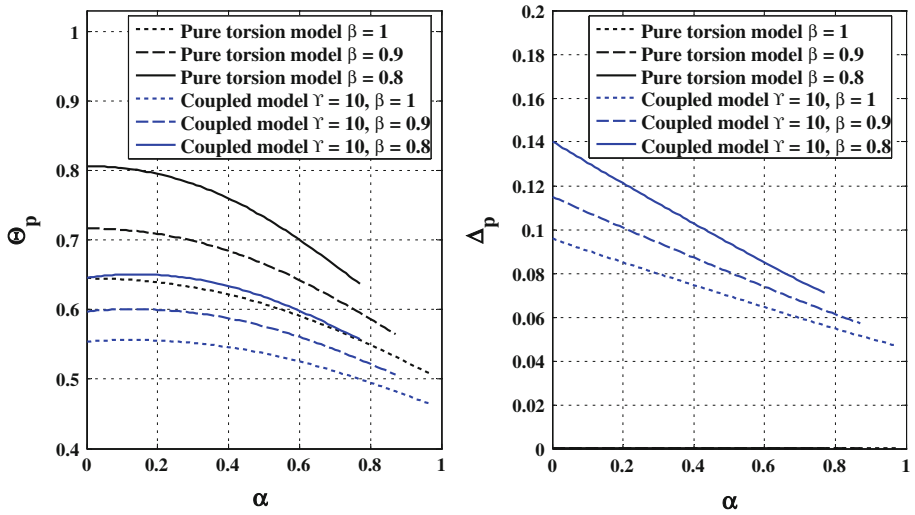

Fig. 4 Effects of α and β on the pull-in angle Θ_p and pull-in displacement Δ_P of the micromirror under capillary force

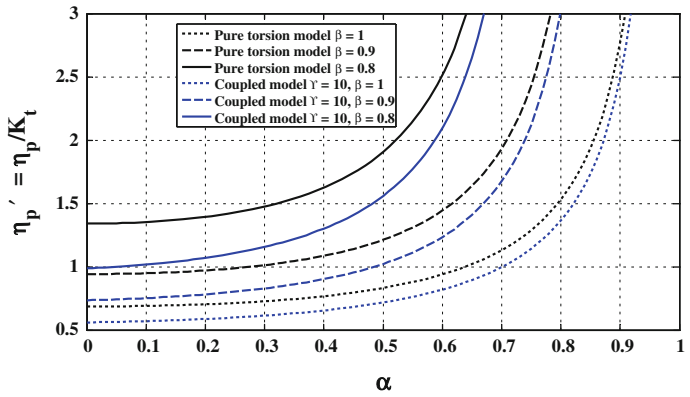

Fig. 5 Effects of α and β on the stability limits of the micromirror under capillary force for both torsion and coupled models

Table 1 Properties of the simulated micromirror

Parameter	Value
G	66 GPa
υ	0.29
L	100 μm
W	100 μm
l	65 μm
t	1.5 μm
w	1.55 μm
l_1	0
l_2	70 μm

curve of the coupled model, it is confirmed that the pure torsion model overestimates the stability limits of the micromirror.

In order to verify the accuracy of the presented model, a group of micromirrors with characteristics given in Table 1 and with different values of h is simulated using the commercial finite element software ANSYS. Figure 6 shows a sample of this group of micromirrors with $h = 41.6\,\mu$m, which has been simulated after applying the capillary force. ANSYS output for deflection of the mirror has been measured and nondimensionalized to be able to be compare it to the results of the coupled model. Figure 7 shows that $\eta' - \Theta$ and $\eta' - \Delta$ characteristics of micromirrors obtained from the coupled model agree well with finite element results, but they considerably differ from those of the torsion model especially at larger values of η'.

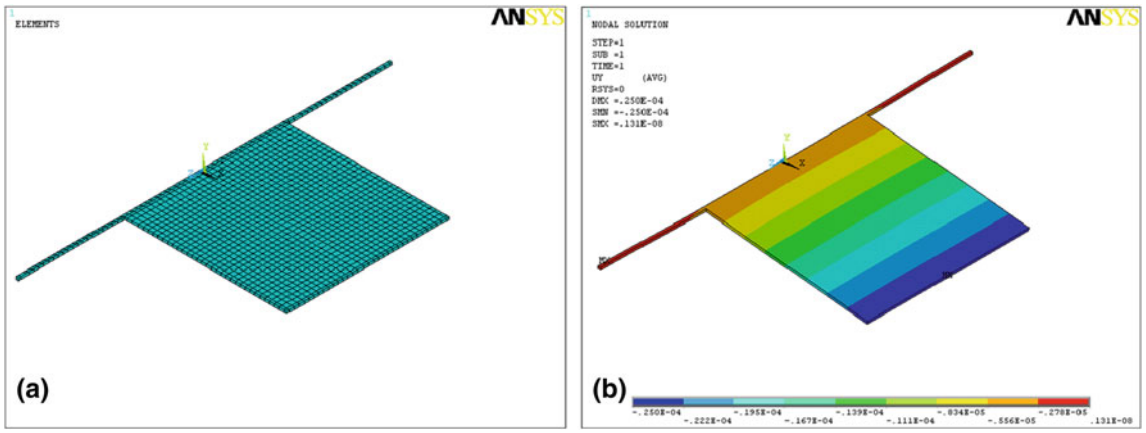

Fig. 6 **a** Meshed configuration of a micromirror with characteristics given in Table 1 and with $h = 41.6\,\mu$m. **b** Deformed configuration of the micromirror shown in Fig. 6a under capillary force

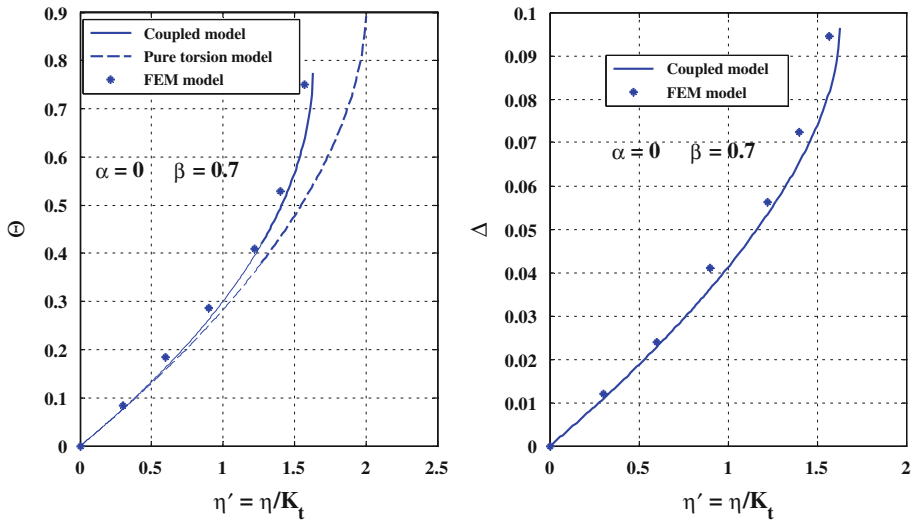

Fig. 7 Equilibrium point of the micromirror shown in Fig. 1 and properties given in Table 1, comparison of the FEM results with the results of the coupled and pure torsion model

4 Conclusion

In the current paper, the effect of bending of the supporting torsion microbeams on the stability limits of micromirrors under capillary force is investigated. The results show that when the bending stiffness is relatively small, the dominant instability mode is the bending mode and under this condition, the torsion model significantly overestimates the stability limits of the micromirror. Furthermore, it is observed that the micromirror response to the capillary force is highly dependent on the bending stiffness of the torsion microbeams, and the presented model is capable of capturing this dependency. Finally, the accuracy of the presented coupled model is verified by comparing its results with finite element results obtained from ANSYS. Results of this paper can be used for a safe, accurate and stable design of micromirrors under wet-etching process where capillary force plays a major role in the fabrication.

Acknowledgments The authors wish to gratefully acknowledge the nameless reviewer for his/her useful comments on this paper. Comparison of the results of the coupled model with the results of an FEM model was his/her suggestion.

References

1. Maluf, N., Williams, K.: An Introduction to Microelectromechanical Systems Engineering, 2nd edn. Microelectromechanical Systems (MEMS) Series. Artech House Inc., Boston (1999)
2. Younis, M.I.: Modeling and simulation of microelectromechanical systems in multi-physics fields. Dissertation submitted to the Faculty of the Virginia Polytechnic Institute and State University in partial fulfillment of the requirements for the degree of Doctor of Philosophy in Engineering Mechanics
3. Chao, P.C.P, Chiu, C.W., Tsai, C.Y.: A novel method to predict the pull-in voltage in a closed form for micro-plates actuated by a distributed electrostatic force. J. Micromech. Microeng. **16**, 986–998 (2006)
4. Hornbeck, L.J.: Spatial light modulator and method. US Patent 5,061,049 (1991)
5. Ford, J.E., Aksyuk, V.A., Bishop, D.J., Walker, J.A.: Wavelength add-drop swiching using tilting micromirrors. J. Lightwave Technol. **17**, 904–911 (1999)
6. Dickensheets, D.L., Kino, G.S.: Silicon-micromachined scanning confocal optical microscope. J. Microelectromech. Syst. **7**(1), 38–47 (1998)
7. Zavracky, P.M., Majumber, S., McGruer, E.: Micromechanical switches fabricated using nickel surface micromachining. J. Microelectromech. Syst. **6**, 3–9 (1997)
8. Toshiyoshi, H., Fujita, H.: Electrostatic micro torsion mirrors for an optical switch matrix. J. Microelectromech. Syst. **5**, 231–237 (1996)
9. Wei, Z., Zhao, Y.P.: Growth of liquid bridge in AFM. J. Phys. D Appl. Phys. **40**(14), 4368–4375 (2007)
10. Van Zwol, P.J., Palasantzas, G., De Hosson, J.Th.M.: Influence of roughness on capillary forces between hydrophilic surfaces. Phys. Rev. E **78**, 03160 (2008)
11. Mastrangelo, C.H., Hsu, C.H.: Mechanical stability and adhesion of microstructures under capillary forces-part I: basic theory. J. Microelectromech. Syst. **2**(1), 33–43 (1993)
12. Mastrangelo, C.H., Hsu, C.H.: Mechanical stability and adhesion of microstructures under capillary forces-part 2: experiments. J. Microelectromech. Syst. **2**(1), 44–55 (1993)
13. Moeenfard, H., Kahrobaiyan, M.H., Ahmadian, M.T.: Aplication of the extended Kantorovich method to the static deflection of microplates under capillary force. In: ASME International Mechanical Engineering Congress and Exposition, IMECE2010-39517 (2010)
14. Zitzler, L., Herminghaus, S., Mugele, F.: Capillary forces in tapping mode atomic force microscopy. Phys. Rev. B **66**, 155436 (2002)
15. Li, X., Peng, Y.: Investigation of capillary adhesion between the microcantilever and the substrate with electronic speckle pattern interferometry. Appl. Phys. Lett. **89**, 234104 (2006)
16. Jang, J., Schatz, G.C., Ratner, M.A.: Capillary force in atomic force microscopy. J. Chem. Phys. **120**(3), 1157–1160 (2004)
17. Guo, J.G., Zhou, L.J., Zhao, Y.P.: Instability analysis of torsional MEMS/NEMS actuators under capillary force. J. Colloid Interface Sci. **331**(2), 458–462 (2009)
18. Huang, J.-M., Liu, A.Q., Deng, Z.L., Zhang, Q.X., Ahn, J., Asundi, A.: An approach to the coupling effect between torsion and bending for electrostatic torsional micromirrors. J. Sens. Actuators A **115**, 159–167 (2004)
19. Rao, S.S.: Vibration of Continuous Systems. Wiley, New Jersey (2007)
20. Bochobza-Degani, O., Nemirovsky, Y.: Modeling the pull-in parameters of electrostatic actuators with a novel lumped two degree of freedom pull-in model. Sens. Actuator A **97–98**, 569–578 (2002)
21. Bochobza-Degani, O., Nemirovsky, Y.: Erratum to "Modeling the pull-in parameters of electrostatic actuators with a novel lumped two degrees of freedom pull-in model [Sensors and Actuators A97–98: 569–578]", Sens. Actuators A **101**, 392 (2002)